DOI: 10.1002/ejic.200701339

Synthesis, X-ray Structure and Reactivity of a Sterically Protected Azobisphenol Ligand: On the Quest for New Multifunctional Active Ligands

Emi Evangelio,[a] Javier Saiz-Poseu,[b] Daniel Maspoch,[b] Klaus Wurst,[c] Felix Busque,*[d] and Daniel Ruiz-Molina*[a,e]

Keywords: Azobisphenol ligand / Acid–base behaviour / Multifunctional ligands / Valence tautomerism / Chromophores

Different synthetic routes have been explored for the synthesis of the sterically protected 2,2′-dihydroxy-4,3,4,3′-tetra-*tert*-butylazobenzene ligand (**2**), which is an excellent candidate for the development of valence tautomeric complexes. As expected, such a ligand exhibits good reactivity with transition-metal ions, as shown by the synthesis and characterization of the new cobalt complex $[\mathrm{Co}(\mathbf{2}^{2-})(\mathrm{H_2O})_3]\mathrm{Cl}\cdot 2.5\mathrm{EtOH}\cdot\mathrm{H_2O}$ (**8**). This fact together with the reversible deprotonation/protonation of the phenol groups has been used to create a chromophoric array of three states with significantly different colours, which can interconvert reversibly between them.

Introduction

There is currently active interest in the development of molecular electronic devices that can be used as optical and/or magnetic data storage media.[1] Compounds of specific interest are bistable molecular materials having two nearly degenerated states with different optical and/or magnetic properties.[2] These complexes have an appreciable sensitivity to the environment so an external perturbation, like photons or temperature, may lead to an interconversion between the two degenerated electronic states. Examples of electronic labile complexes are valence tautomeric complexes.[3] Valence tautomeric metal complexes with at least two redox-active centres, the metal ion and an electroactive ligand, are characterized by the existence of two electronic isomers (valence tautomers).[4] The interconversion between the two electronic isomers is accomplished by a reversible intramolecular electron transfer involving the metal ion and the redox-active ligand. Interestingly, each isomer exhibits different charge distributions, and consequently, different optical, electric and magnetic properties.[5]

Ligands that display different oxidation states when coordinated to metallic centres have been broadly studied by both theoretical[6] and experimental means.[7] However, we must emphasize that even though the number of redox-active ligands is considerable, those exhibiting valence tautomerism are rather limited since they must simultaneously satisfy two conditions: (i) the degree of covalency in the interaction between the metal ion and electroactive ligand must be low, and (ii) the energy of their frontier orbitals must be similar.[8]

Most of the complexes that so far have shown to exhibit valence tautomerism are transition-metal complexes of quinone or quinone-based ligands.[9] Nevertheless, the number of electroactive ligands inducing valence tautomerism is expanding with the inclusion of new electroactive ligands such as tetraphenylporphyrin,[10] polychlorotriphenylmethyl[11] and phenoxyl radicals.[12] Among them, phenoxyl radicals are monovalent oxygen radical species that exhibit delocalization of the unpaired electron over the aromatic ring with *ortho* and *para* substituents that give steric protection.[13] Several groups have prepared metal–phenoxylate complexes, which give new insights into the chemical factors that govern the generation and stability of this type of radical.[14] It is worth mentioning the work developed by Wieghardt et al; they established that bidentate *O*,*N*-coordinated *o*-aminophenolato ligands can be found in different protonation and oxidation levels: *o*-imidophenolate(2–) anions, *o*-iminobenzosemiquinonate(1–) radical monoanions or even *o*-iminobenzoquinone. All these forms can exist in coordination compounds, as confirmed by low-temperature X-ray crystallography.[15] A further step has been the study and characterization of *O*,*N*,*O*-coordinated ligands containing two phenolate donor groups, such as 2-[(3,5-bis(1,1-dimethylethyl)-6-hydroxyl-2,4-cyclohexadien-1-ylidene)amino]-4,6-bis(1,1-dimethylethyl)phenol (**1**).[16] These ligands, in addition to producing phenoxyl radicals in the presence of air, exhibit better chelating capabilities and good π-donor

---

[a] Institut de Ciència dels Materials de Barcelona (CSIC),
Esfera UAB, 08193 Bellaterra, Catalonia, Spain
[b] Institut Català de Nanotecnologia,
Campus UAB, 08193 Bellaterra, Catalonia, Spain
[c] Institut für Allgemeine Anorganische und Theoretische Chemie, Universität Innsbruck,
Innrain 52a, Innsbruck, Austria
[d] Chemistry Department, Universitat Autònoma de Barcelona,
Campus UAB, 08193 Bellaterra, Catalonia, Spain
[e] Centre de Nanociència i Nanotecnologia,
Campus UAB, 08193 Bellaterra, Catalonia, Spain
Fax: +34-935814777
E-mail: dani@icmab.es

atoms that stabilize higher oxidation states, a fact that has allowed the observation of valence tautomerism in some of their complexes.[17]

The advantages of the valence tautomeric complexes obtained from the Schiff base ligand **1** over transition-metal complexes with *o*-quinone ligands are considerable. First, valence tautomeric Schiff base complexes display higher stabilities in atmospheric oxygen in solution and in the solid state.[18] Second, the differences between the optical properties of the isomers involved in the valence tautomerism of the cobalt Schiff base complex are enhanced relative to those observed for cobalt complexes with *o*-quinone ligands. Third, the Schiff base ligand exhibits a richer electrochemical behaviour since it can exist in different oxidation forms, ranging from +1 to –3, which may lead to stable coordination complexes with several metal ions in a variety of oxidation states.[19]

Because of the interest in this family of ligands, we focused our attention on obtaining new bisphenol ligands similar to **1**, particularly bearing additional functional groups that can add a multifunctional character to the valence tautomeric behaviour. For this, 2,2′-dihydroxy-4,3,4,3′-tetra-*tert*-butylazobenzene (**2**) would be an excellent candidate. While keeping the same coordination capability and steric protection of the radicals through the presence of *tert*-butyl groups, the incorporation of the azo group ensures a multifunctional character thanks to their wide spread application as dyes, acid–base indicators and histological stain applications, among others.[20] Moreover, the possibility to use azo compounds as electron–acceptor or radical ligands in transition-metal species has already been reported.[21] However, in spite of its interest, reports on **2** have so far been scarce – there is a report on a Cu^{II} complex obtained as a side product[22] and on a cumbersome and harsh low-yield synthesis.[23]

Herein we report on the exploration of several new synthetic routes for the synthesis of azobisphenol **2**, and include the one-pot synthesis of a related Co^{III} complex. In addition, both its acid–base character based on the presence of the phenol groups and its reactivity with transition-metal ions has been used to develop a chromophoric sensor. This fact adds value to the synthesis of **2** since the colour change of chromogenic sensors provides an informative and important signal for its use in analyte-sensing, environmental and biomedical applications.[24]

Results and Discussion

Synthesis of 2

In the present work, four different synthetic approaches for the synthesis of azobisphenol **2** were initially envisaged.[25–28] Our first synthetic trials toward the synthesis of **2** (Scheme 1) were done following three different routes,[26–28] without any success. When nitro derivative **3** was exposed to reductive coupling conditions, either with $LiAlH_4$[26a] or with the $Pb^0/HCOONH_4$ system,[26b] no desired diazo product **2** was obtained, and only the starting material and aniline **4** were recovered. Similarly, oxidative coupling of aniline **4** with cetyltrimethylammonium dichromate[27] failed, and degradation products were obtained. The *tert*-butylation reaction[28] of 2,2′-dihydroxy-azobenzene was also tested, though no traces of the desired product were obtained.

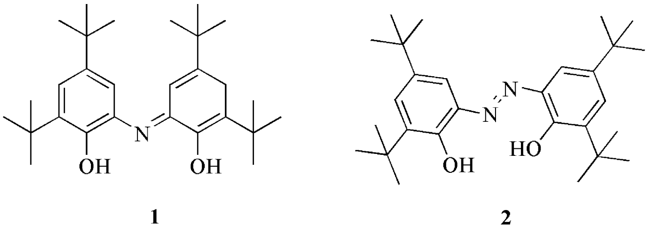

Scheme 1. Molecular structures of **1** and **2**.

Fortunately, an alternative synthetic route, which in fact is the most extended synthetic strategy for the synthesis of this type of compounds,[25] was most successful (see Scheme 2). Initially, nitrophenol **3** was obtained in a 73% yield by nitration of phenol **5** following a modified experimental route previously described.[29] The reaction was performed at about –20 °C to avoid the side dinitration reaction. Compound **3** was then reduced by using Pd/C in methanol[30] to afford aniline **4** in an 84% yield. Finally, the coupling reaction[25] of the diazonium salt **6**, derived from aniline **4** with phenol **5**, afforded the diazo derivative **2** in 21% yield. This last reaction was performed under slightly basic or neutral conditions to avoid conversion of the diazonium salt to the corresponding diazohydroxide compound.

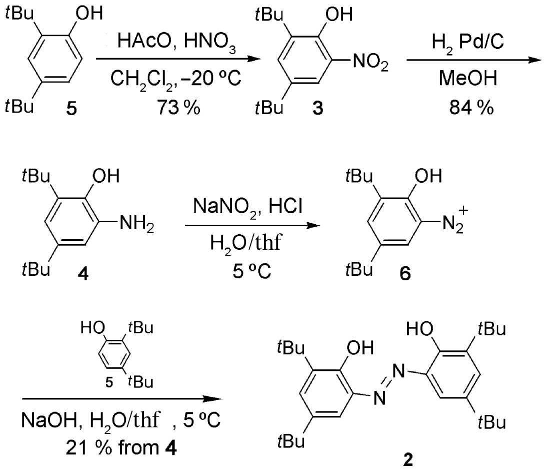

Scheme 2. Route for the synthesis of **2**.

Crystal Structure of 2

The molecular and crystal structure of **2** was investigated by X-ray single crystal analysis. The crystallographic data and experimental parameters are summarized in Table 4. Selected bond lengths and angles are also given in Table 1. Molecule **2** crystallizes in the *C*2/*c* monoclinic space group, and the cell parameters are reported in Table 4. An ORTEP view of **2** is shown in Figure 1. The high molecular symmetry is reflected by the presence of an inversion centre, which leads to a *trans* geometry of the hydrazone group with respect to both quinone moieties. This configuration seems to be favoured by two intramolecular hydrogen bonds between O1–H···N1 with distances of 1.695 Å and angles of 148.6°.

Table 1. Selected bond lengths [Å] and angles [°] for **2**.

Bond lengths			
N1–N1′	1.280(2)	O1–C1	1.357(1)
N1–C2	1.406(2)		
C1–C2	1.406(2)	C4–C5	1.406(2)
C2–C3	1.401(2)	C5–C6	1.390(2)
C3–C4	1.373(2)	C6–C1	1.498(2)
Angles			
C2–N1–N1′	117.1(1)		
O1–C1–C2	120.7(1)		
C1–C2–N1	125.1(1)		

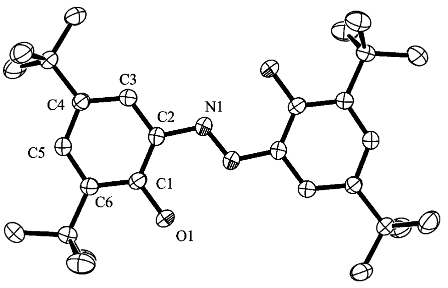

Figure 1. ORTEP drawing of the azobisphenol **2** at the 30% probability level. Hydrogen atoms have been omitted for clarity.

Acid–Base Equilibria of 2

The acid–base activity of azobisphenol **2** was investigated by means of UV/Vis absorption spectroscopy. An ethanol solution of **2** displays two intense broad absorption bands at 347 nm, most likely assigned to the n–π* transition of the azo (N=N) group, and at 453 nm associated with the presence of the hydroxyl groups. Both bands are expected to be sensitive and to change upon acid/base addition, especially in the case of the second band.[31]

Figure 2 displays the changes measured in the absorption spectrum of an ethanol solution of **2** (C_0 = 5.7 × 10^{-5} M) upon addition of base [80 μL of tetrabutylammonium hydroxide (tba) C_0 = 4.3 × 10^{-3} M]. As the pH increases, the intensity of the band at 347 nm associated with the n–π* transition decreases . However, a new band at 520 nm appears, and the intensity of the initial peak at 453 nm, associated with the hydroxyl groups, decreases until the band almost disappears. Deprotonation of the phenol groups under basic conditions leads to a charge density shift and consequently a bathochromic shift of the new band, which is accompanied by a colour change from yellow to violet. The clean isosbestic point at 493 nm also indicates an equilibrium between the acid (**2**) and the basic (**2**$^{2-}$) form of this molecule (Figure 2a), which most likely takes place through the formation of the monoanionic form. Finally, it is important to emphasize that this process is fully reversible upon addition of acid (HCl), and therefore the absorption spectrum of the neutral form **2** and the yellow colour of the solution can be recovered. In any case, protonation of the azo group was not detected after addition of controlled amounts of acid.

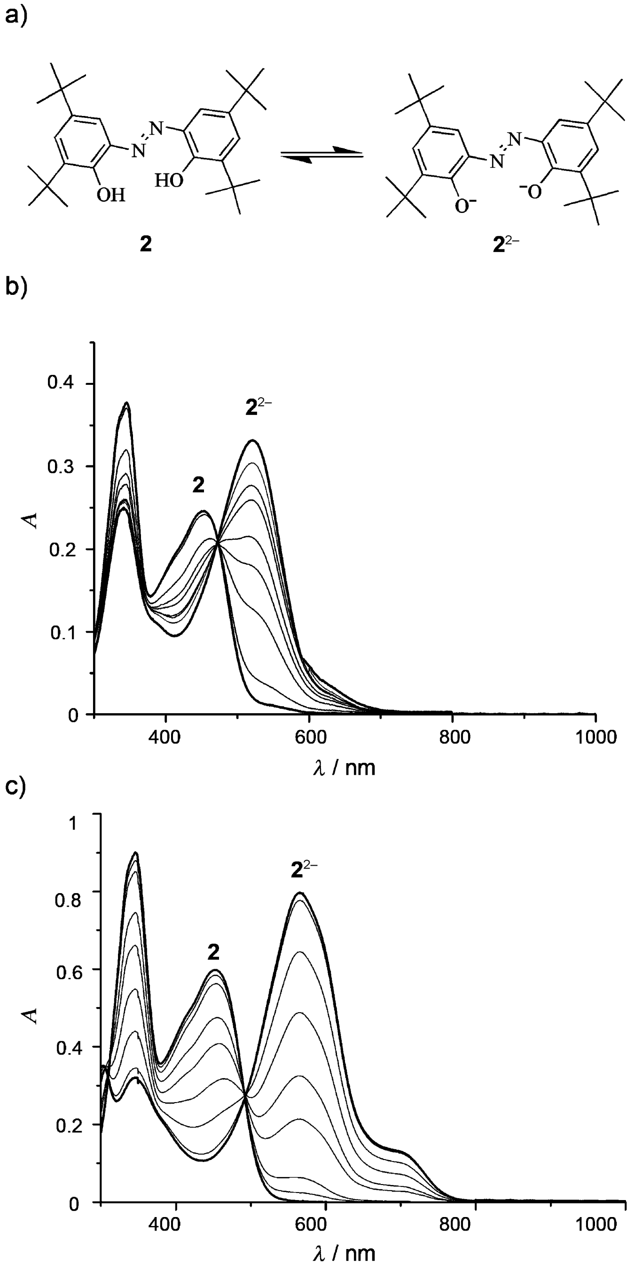

Figure 2. (a) Schematic representation of the acid–base equilibrium of **2**. (b) UV/Vis spectra of **2** (0.057 mM) in ethanol as the pH increases. (c) UV/Vis spectra of **2** (0.057 mM) in thf as the pH increases. In (b) and (c) each line corresponds to the addition of 40 μL of tba (0.4 mM) until total deprotonation of **2** occurs. The process is fully reversible upon addition of HCl.

The acid–base activity of **2** was also investigated in thf solution (Figure 2c). In this solvent, the spectrum of **2** also displays the two intense broad absorption bands at 347 nm and 453 nm, with no significant solvatochromic shift. Upon addition of base, deprotonation of the phenol groups takes place, as described previously for the ethanol solution, which leads to the appearance of a new band at 565 nm, and the intensity of the initial peak at 453 nm decreases. However, two main differences can be noted: (i) a solvatochromic effect is detected in the absorbance spectra for the $\mathbf{2}^{2-}$ species (the spectral parameters for the species **2** and $\mathbf{2}^{2-}$ are summarized in Table 2), which could be tentatively ascribed to changes in solvent polarity as well as in the solvent hydrogen-bond-accepting capacity,[32] and (ii) the intensity of the band at 347 nm decreases more considerably.

Table 2. UV/Vis spectroscopic data for the species **2** and $\mathbf{2}^{2-}$ in ethanol and thf solutions.

State	Solvent	λ [nm]	ε [$\mathrm{M}^{-1}\,\mathrm{cm}^{-1}$]
2	EtOH	347, 453	13899, 9322
$\mathbf{2}^{2-}$		347, 520	7834, 11624
2	thf	347,453	15789, 10488
$\mathbf{2}^{2-}$		347, 565	5623, 14348

Complexation Ability of 2

The complexation ability of **2** with transition-metal ions such as $\mathrm{Co^{II}}$ was initially studied in solution (Figure 3a). First, the deprotonated form $\mathbf{2}^{2-}$ was obtained after an ethanol solution of **2** (3 mL, $C_0 = 1\times10^{-5}$ M) was made basic with tba (5 μL, $C_0 = 5\times10^{-2}$ M), as confirmed by UV/Vis spectroscopy. An aqueous solution of $\mathrm{CoCl_2{\cdot}6H_2O}$ (25 μL, $C_0 = 9\times10^{-4}$ M) was then added. Immediately, the intensity of the band at 520 nm, characteristic of the $\mathbf{2}^{2-}$ form, started to decrease and that of the new band at 560 nm with two shoulders at 520 and 484 nm, associated with the formation of the corresponding cobalt complex **2·Co**, increases. The appearance of the new band is accompanied by a colour change from violet to red–purple. The complexation ability of ligand **2** was also tested by direct reaction of **2** with an ethanol solution of cobalt acetate, whose basic character is expected to deprotonate the azobisphenol ligand. The UV/Vis spectra of an ethanol solution of **2** upon addition of cobalt acetate are shown in Figure 3b. Addition of a solution of $\mathrm{Co(CH_3COO)_2{\cdot}4H_2O}$ (240 μL, $C_0 = 1\times10^{-3}$ M) to the ethanol solution of **2** ($C_0 = 5.5\times10^{-5}$ M) also induces a shift in the band at 453 nm, which is characteristic of **2**, to 560 nm. The shoulders at 520 and 484 nm arise as a result of the formation of the complex **2·Co**. As expected, the acetate counterion of the metal salt is sufficiently acidic to deprotonate the azo ligand, which leads to the formation of complex **2·Co**. Moreover, the process is fully reversible on addition of acid (HCl) and the absorption spectrum of the neutral form **2** is thus recovered, and consequently, the yellow colour of the solution.

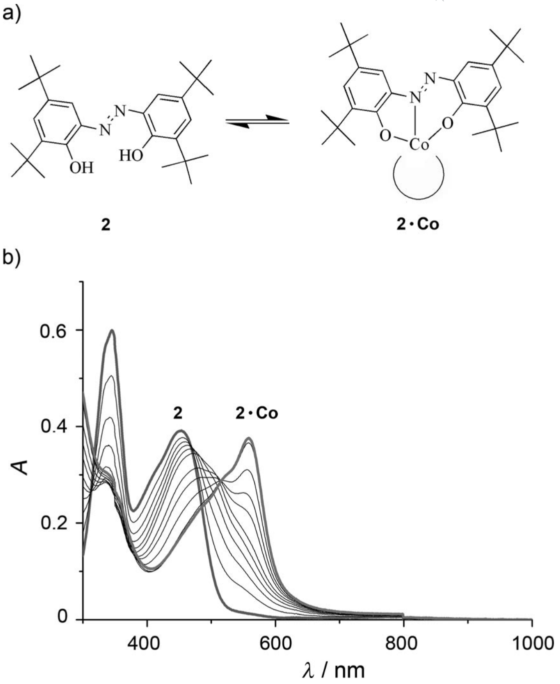

Figure 3. (a) Schematic representation of the complexation equilibrium of **2**. (b) UV/Vis spectra of **2** (0.057 mM) in the presence of $\mathrm{Co(CH_3COO)_2{\cdot}4H_2O}$ (1 mM), added at regular intervals of 24 μL.

To shed more light into the reactivity of ligand **2** and the nature of the complex formed upon reaction with a cobalt salt, we considered the straight chemical synthesis of a transition-metal complex bearing ligand **2**. For this, we were inspired by the methodology described by Pierpont[17a] and Dei et al.[17b] for the synthesis of transition-metal complexes bearing ligand **1**. These authors showed that 3d metal ions react with 3,5-di-*tert*-butylcatechol (3,5-DTBCatOH) and aqueous ammonia in the presence of air to yield complexes of the Schiff base bisquinone ligand. Moreover, for the case of the copper metal ion, excess ammonia induces a redox cascade reaction coupled with air oxidation, which is responsible for the formation of a related azophenolate complex.[22] By taking these precedents into account, and only after several different reaction trials did the reaction of 3,5-DTBCatOH (6 equiv.), ammonia (excess) under aerobic conditions and a mixture EtOH/$\mathrm{H_2O}$ (50:50) and $\mathrm{CoCl_2{\cdot}6H_2O}$ (1 equiv.) yield complex $[\mathrm{Co}(\mathbf{2}^{2-})(\mathrm{H_2O})_3]\mathrm{Cl{\cdot}2.5EtOH{\cdot}H_2O}$ (**8**), as characterized by X-ray diffraction and chemical analysis (vide infra). Most likely, the reaction mechanism takes place through the formation of complex [Co(Cat-N-SQ)(Cat-N-BQ)], where (Cat-N-BQ)^{-} and (Cat-N-SQ)^{2-} refer to the monoanionic and dianionic forms of ligand **1**, respectively. Indeed, upon addition of excess concentrated aqueous ammonia to a solution of 3,5-DTBCatOH and $\mathrm{CoCl_2{\cdot}6H_2O}$, the solution turned dark violet, characteristic of the formation of [Co(Cat-N-SQ)(Cat-N-BQ)]. However, after 10 min whilst stirring, the solution gradually became a lighter violet colour and finally the characteristic red–purple colour of complex **8**. After 4 h of stirring, the solution was filtered and a purple compound was obtained, which was characterized by chemical analysis as complex [Co(Cat-NSQ)(Cat-N-BQ)]. This result partially confirms the formation of this species as an intermediate along the reaction. The solution was then kept for 2 h, and crystals of complex **8** suitable for X-ray analysis were collected.

Crystallographic data and experimental parameters used for the resolution of the X-ray structure of **8** are summarized in Table 4. Selected bond lengths and angles are given in Table 3. Complex **8** crystallizes in the $P\bar{1}$ triclinic space group with the cell parameters as reported in Table 4. An ORTEP drawing is shown in Figure 4. The asymmetric unit contains one molecule of **8**, one chloride counterion, two and a half ethanol molecules and one water molecule of crystallization. The cobalt ion displays an octahedral coordination geometry by binding to two oxygen and one nitrogen atoms of **2**$^{2-}$ and three water molecules. The Co1–O1, Co1–O2, Co1–N1 distances are 1.868(4), 1.856(4) and 1.849(6) Å, respectively, so **2**$^{2-}$ is a tridentately coordinated to the cobalt ion. In this coordination mode, the azobisphenolate ligand forms both typical five- and six-membered chelate rings with the cobalt atom. All bond lengths and angles are characteristic of and similar to those previously reported for other azobisphenolate-based complexes.[22]

Table 3. Selected bond lengths and angles for **8**.

Bond lengths			
Co1–O1	1.868(4)	Co1–O2	1.856(4)
Co1–N1	1.849(6)	N1–N2	1.266(8)
N1–C2	1.422(8)	N2–C8	1.386(9)
O1–C1	1.334(8)	O2–C7	1.326(8)
C1–C2	1.391(10)	C7–C8	1.417(10)
Angles			
O1–Co1–O2	177.0(2)	O1–Co1–N1	86.6(2)
O2–Co1–N1	96.1(2)	N1–Co1–O3	88.9(3)
C2–N1–N2	118.4(6)	C8–N2–N1	119.9(6)
N1–Co1–O5	177.6(2)		

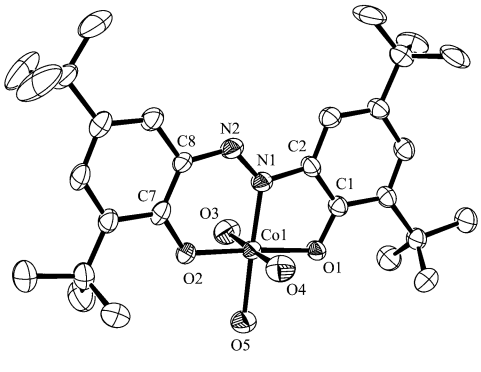

Figure 4. ORTEP drawing of the azobisphenol–Co complex **8** at the 30 % probability level. Hydrogen atoms, the chloride counterion and the solvent molecules are omitted for clarity.

Elemental analysis and electrospray–(+) measurements in methanol of a polycrystalline sample of **8** are in agreement with the structure previously described (see Experimental Section). The FTIR spectrum (KBr pellet) of **8** exhibits peaks at 1268 and 1450 cm^{-1}, which are characteristic of the ν(C–O) and ν(N=N) modes.[31]

The ν(O–H) mode for the three coordinated water molecules appears as a broad band from 3300–3100 cm^{-1}. The electronic spectra in ethanol consists of an intense band with a maximum at 553 nm (1.2×10^4 M^{-1}cm^{-1}) and two shoulders at 512 and 476 nm. Interestingly, these bands are similar to those observed for **2·Co** in solution, which confirms the series of experiments as described in Figure 3. For comparison purposes, the electronic spectrum of complex **8** was also monitored in two additional solvents. The most intense band shifts its maxima to 560 nm (7.4×10^3 M^{-1}cm^{-1}) in thf and to 565 nm (6.2×10^3 M^{-1}cm^{-1}) in toluene. The shoulders shift to 523 and 489 nm in thf and 529 and 492 nm in toluene, respectively, which confirms the existence of a solvatochromic effect as described previously for compound **2**$^{2-}$. In addition, the ^{1}H NMR spectra of deuterated methanol solutions of **2·Co** and **8** also suggest that both complexes are almost identical. Indeed, as described in the Experimental Section, the signals attributed to the four *tert*-butyls groups and the four aromatic protons are very similar, with small shift differences that are expected according to the different coordination environments of the Co^{III} ion in **2·Co** and **8**.

The magnetization temperature dependence data in the temperature range 5–300 K under an external applied magnetic field of 0.5 T exhibits diamagnetic behaviour along the whole temperature range. These results are consistent with the formulation of the ligand in the form of diamagnetic azophenolate (**2**$^{2-}$) and Co^{III} ions. The extra positive charge is compensated for by the presence of the chloride anion. This charge assignment was also confirmed by cyclic voltammetry. Cyclic voltammetry of complex **8** shows two reversible one-electron waves at +1.093 V, which is assigned as an oxidation ligand-centred process, and at –1.083 V, which is assigned to the reduction of Co^{III} to Co^{II} or, to a lesser extent, of a ligand-centred process.

Finally, the redox activity of ligand **2** described previously inspired us to explore the possible existence of valence tautomerism for complex **8** by means of variable-temperature UV/Vis spectroscopy in the 280–370 K temperature range. An external stimuli such a temperature may induce a reversible intramolecular electron transfer between the redox-active ligand and the metal ion. However, in spite of the different solvents and solvent mixtures used, no valence tautomerism could be detected for **8**. In all cases, a large reduction in the intensity of the bands, followed by the appearance of new bands at very short wavelengths, is observed. This behaviour has been attributed to the decomposition of the complex under the experimental conditions, as confirmed by the irreversibility of the process.

Three-State Switching Array

The studies described previously confirmed the suitability of **2** to create a chromophoric array of three states with significantly different colours, thanks to the presence of the azo group, which can interconvert reversibly between them by means of acid/base and complexation reactions. The UV/Vis spectra of the three species **2**, **2**$^{2-}$ and **2·Co** and a schematic representation of the different mechanisms that can be followed to interconvert between them are shown in Figure 5. The yellow colour of **2** changes to violet and red–purple upon addition of a base such as tba and $Co(Cl)_2\cdot 6H_2O$, respectively. In the first case, the dianionic compound $\mathbf{2}^{2-}$ is formed, whereas addition of the cobalt salt induces the formation of the **2·Co** complex. In both cases, subsequent addition of HCl leads to **2**, which shows that the process is fully reversible. The colour changes can nicely be detected by the naked eye, as shown in Figure 5a. This fact was also observed for complex **8**. Upon addition of HCl to an ethanol solution of complex **8**, crystals of pure **2** (40% yield) were obtained by recrystallization from the solution, which opens an alternative high-yield methodology for obtaining **2** to those described in the previous section. Finally, the reverse reaction, i.e. addition of further base to the acidic solution of **2** and the free cobalt ion did not process. For this process to work, further addition of $Co(CH_3COO)_2\cdot 4H_2O$ is necessary.

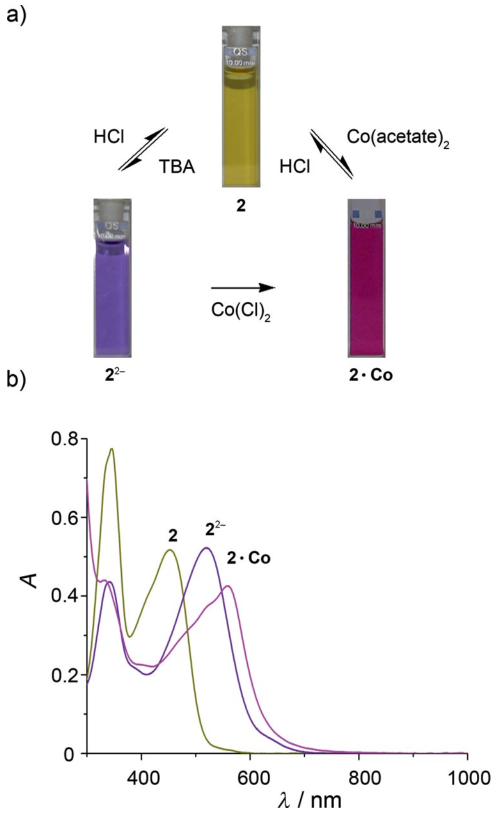

Figure 5. (a) Schematic representation of the three-state switching array. (b) UV/Vis spectra of an ethanol solution of **2** (0.055 mM) with the initial addition of 20 µL tba (0.8 M) to generate $\mathbf{2}^{2-}$ and subsequent addition of 240 µL of $Co(Cl)_2\cdot 6H_2O$ (1 mM) to generate **2·Co**.

Conclusions

A new synthetic route for the synthesis of the sterically protected azobisphenol **2** has been described. The reversible deprotonation/protonation of the phenol groups has been shown to take place under basic and acidic conditions, respectively. Moreover, ligand **2** exhibits good reactivity with transition-metal ions such as cobalt, as shown UV/Vis spectroscopy in solution. Both the acid–base character and the complexation ability of **2** have been used to create a chromophoric array of three states (**2**, $\mathbf{2}^{2-}$ and **2·Co**) with significantly different colours (enhanced by the presence of the azo group), which can interconvert reversibly between them. The reactivity of ligand **2** has also been used to prepare complex **8**, although no evidence of valence tautomerism was detected. Further work is currently underway to prepare a new series of complexes bearing this ligand with different *N,N′* counter ligands, which will allow us to study valence tautomerism.

Experimental Section

All reagents were purchased from Aldrich Chemical Co. and used as received. The solvents were dried by distillation over the appropriate drying agents. All reactions were performed avoiding moisture by standard procedures and under an atmosphere of nitrogen and monitored by analytical thin-layer chromatography (TLC) by using silica gel 60 F_{254} pre-coated aluminium plates (0.25 mm thickness). Flash column chromatography was performed using silica gel 60 Å, with particle sizes 35–70 µm.

Synthesis of 2,2′-Dihydroxy-4,3,4′,3′-tetra-*tert*-butylazobenzene: A solution of sodium nitrite (0.027 g, 0.40 mmol) in a mixture of water (0.2 mL) and 35% HCl acid (0.1 mL, 0.90 mmol) was first cooled to 5 °C. A thf solution (0.6 mL) of aniline **4** (0.080 g, 0.36 mmol) was then added, and the resulting mixture was stirred at 5 °C for 20 min. This solution was then added dropwise to another solution of compound **5** (0.075 g, 0.36 mmol) and NaOH (0.036 g, 0.90 mmol) in a mixture of thf (0.5 mL) and water (0.5 mL). The whole mixture was stirred at 10 °C for 30 min, adjusted to a pH of 6–7 and extracted with ethyl acetate (3 × 10 mL). The entire organic extracts were dried with magnesium sulfate, filtered and concentrated under reduced pressure to yield an oil that was chromatographed through silica gel by using a mixture of ethyl acetate/ethyl ether (15:1) to afford 0.033 g of azobisphenol **2** (0.08 mmol, 21% yield). FTIR (KBr): $\tilde{\nu}$ = 3428 [ν(O–H)], 2963, 2905, 2862 [ν(C–H)], 1613, 1479, 1461, 1428 [ν(N=N)]), 1393, 1360, 1266 [ν(C–O)], 1249, 1220, 1197, 1169 cm^{-1}. $C_{28}H_{42}N_2O_2$ (438.31): calcd. C 76.0, H 9.5, N 6.4; found C 75.9, H 9.5, N 6.3. ES–(+) (MeOH): *m/z* = 439 [M^+, $C_{28}H_{43}O_2N_2$]. ^1H NMR (400 MHz, [D_8]toluene): δ = 1.46 (s, 18 H, CH_3), 1.81 (s, 18 H, CH_3), 7.67–7.72 (m, 4 H, aromatic H), 13.70 (s, 2 H, OH) ppm.

Synthesis of Complex 2·Co: An ethanol solution (20 µL) of $Co(CH_3COO)_2\cdot 4H_2O$ (28 mg, 0.11 mmol) was added to an ethanol solution (0.75 mL) of 2,2′-dihydroxy-4,3,4′,3′-tetra-*tert*-butylazobenzene (**2**) (1.3 mg, 0.003 mmol) in the NMR tube, whilst stirring. The colour of the mixture turned to a lighter violet colour, and the obtention of the product was followed by ^1H NMR spectroscopy. ^1H NMR (400 MHz, [D_4]MeOH): δ = 1.41 (s, 18 H, CH_3), 1.62 (s, 9 H, CH_3), 1.66 (s, 9 H, CH_3), 7.35 (s, 1 H, aromatic H), 7.49 (s, 1 H, aromatic H), 7.77 (s, 1 H, aromatic H), 8.10 (s, 1 H, aromatic H) ppm.

Synthesis of Complex 8: An ethanol solution (25 mL) of 3,5-di-*tert*-butylcatechol (5 g, 23 mmol) was added to an aqueous solution

(25 mL) of $CoCl_2·6H_2O$ (6.2 g, 26 mmol) whilst stirring. Immediately, an aqueous solution (25 mL) of ammonia was added. The colour of the mixture turned to dark violet, which changed to a lighter violet colour after 10 min whilst stirring. The mixture was then stirred for a further 4 h, and after filtration, crystals of **8** were collected from the solution. FTIR (KBr): $\tilde{\nu}$ = 3109 [$\nu(H_2O)$], 2955, 2905, 2866 [ν(C–H)], 1612, 1480, 1438, 1360, 1278, 1254, 1162 cm^{-1}. $C_{28}H_{52}ClCoN_6O_5$ (646.69): calcd. C 51.4, H 8.5, N 12.8; found C 50.3, H 7.9, N 12.6. ES–(+) (MeOH): *m/z* = 512 [M^+, $C_{28}H_{41}CoN_2O_3$]. ^1H NMR (400 MHz, [D$_4$]MeOH): δ = 1.347 (s, 9 H, CH_3), 1.353 (s, 9 H, CH_3), 1.44 (s, 9 H, CH_3), 1.48 (s, 9 H, CH_3), 7.29 (s, 1 H, aromatic H), 7.34 (s, 1 H, aromatic H), 7.70 (s, 1 H, aromatic H), 8.15 (s, 1 H, aromatic H) ppm.

Physical Measurements: Microanalyses were performed by the Servei d′Analisi of the Universitat Autònoma de Barcelona. Electronic absorption spectra were recorded with a Varian Cary05e spectrophotometer equipped with a thermostatted cell holder that can operate between 280 K and 370 K. The stability of the temperature was better than ±5 K. Spectra were collected on samples that were previously thermally equilibrated at each temperature for 10 min. Magnetic susceptibilities of both samples were measured in the temperature range 1.8–350 K with a Quantum Design MPMS®XL superconducting SQUID magnetometer operating at a magnetic field strength of 0.1 T. The paramagnetic susceptibility was corrected for the holder capsules and the tabulated Pascal constants. Cyclic voltammograms were recorded with a Perkin–Elmer instrument at 20 °C in CH_3CN solution containing 0.10 M commercial tetrabutylammonium hexafluorophosphate as supporting electrolyte, with a glassy carbon working electrode and an Ag/AgCl reference electrode. Ferrocene was used as an internal standard, and potentials are referenced versus the ferrocinium/ferrocene couple (Fc/Fc$^+$). NMR experiments were performed at the Servei de Ressonància Magnètica Nuclear of the Universitat Autònoma de Barcelona. ^1H NMR spectra were recorded on Bruker DPX250 (250 MHz) and Bruker ARX400 (400 MHz) spectrometers. Proton chemical shifts are reported in ppm ($CDCl_3$, δ = 7.26 or [D$_6$]-DMSO, δ = 2.50 ppm). Infrared spectra were recorded on a Sapphire-ATR Spectrophotometer; peaks are reported in cm^{-1}. High resolution mass spectra (HRMS) were recorded at Micromass-AutoSpec using (ESI+ or ESI–).

Table 4. Crystallographic data for azobisphenol (**2**) and [Co(**2**$^{2-}$)$(H_2O)_3$]Cl·2.5EtOH·H_2O (**8**).

	2	**8**
Formula	$C_{28}H_{42}N_2O_2$	$C_{33}H_{63}N_2O_{8.50}CoCl$
M_W	438.64	718.23
Color	yellow plates	red plates
Crystal system	monoclinic	triclinic
Space group	$C2/c$	$P\bar{1}$
a [Å]	19.4693(2)	10.9158(4)
b [Å]	6.2499(3)	14.2039(5)
c [Å]	21.6187(7)	14.8742(6)
α [°]		101.344(2)
β [°]	91.939(2)	103.320(2)
γ [°]		99.697(2)
V [Å^3]	2629.08(15)	2144.38(14)
Z	4	2
T [°C]	–40(2)	–40(2)
λ [Å]	0.71073 (Mo)	0.71073 (Mo)
$D_{calcd.}$ [mg m^{-3}]	1.108	1.112
μ [mm^{-1}]	0.069	0.506
R, R_w[a]	0.0393, 0.1021	0.0694, 0.1802

[a] $R = \Sigma||F_o| - |F_c||/\Sigma|F_o|$. $R_w = [\Sigma w(|F_o| - |F_c|^2/\Sigma w(F_o)^2]^{1/2}$.

X-ray Data and Structure Determination of 2 and 8: Data collection was performed on a Nonius Kappa CCD equipped with graphite-monochromatized Mo–K_α radiation (λ = 0.71073 Å) and a nominal crystal-to-area-detector distance of 36 mm. Intensities were integrated by using DENZO and scaled with SCALEPACK. Several scans in ϕ and ω direction were made to increase the number of redundant reflections, which were averaged in the refinement cycles. This procedure replaces, in a good approximation, an empirical absorption correction. The structures were solved with direct methods SHELXS86 and refined against F^2 SHELX97. The crystallographic data for compounds **2** and **8** are listed in Table 4. CCDC-682913 and -682914 contain the supplementary crystallographic data for this paper. These data can be obtained free of charge from The Cambridge Crystallographic Data Centre via www.ccdc.cam.ac.uk/data_request/cif.

Acknowledgments

This work was supported by the European Network of Excellence MAGMANet through the project MAT2006-13765-C02. F. B. and D. M. thank the Ministerio de Ciencia y Tecnología and the European Regional Development Fund for a RyC contract. E. E. thanks the Ministerio de Ciencia y Tecnología for a pre-doctoral grant. The authors also thank J. M. Pérez for the magnetic measurements and A. Bernabe for the spectroscopic measurements.

---

[1] a) A. C. Benniston, P. R. Mackie, in *Handbook of Nanostructured Materials and Nanotechnology: Concise Edition* (Ed.: H. S. Nalwa), John Wiley & Sons, San Diego, California, **2001**, p. 693–747; b) P. F. Barbara, *Acc. Chem. Res.* **2001**, *34*, 409, and reviews within.

[2] a) O. Sato, J. Tao, Y.-Z. Zhang, *Angew. Chem. Int. Ed.* **2007**, *46*, 2152–2187; b) H. Tian, S. Yang, *Chem. Soc. Rev.* **2004**, *33*, 85–97; c) A. Beyeler, P. Belser, *Coord. Chem. Rev.* **2002**, *230*, 28–38; d) L. Fabbrizzi, L. Prodi, *Chem. Soc. Rev.* **1995**, *24*, 197–202; e) J.-P. Launay, *Chem. Soc. Rev.* **2001**, *30*, 386–397.

[3] E. Evangelio, D. Ruiz-Molina, *Eur. J. Inorg. Chem.* **2005**, *15*, 2957–2971.

[4] D. A. Shultz, "Valence Tautomerism in Dioxolene Complexes of Cobalt" in *Magnetism: Molecules to Materials II. Molecule-Based Materials* (Eds.: J. S. Miller, M. Drillon), Wiley-VCH, New York, **2001**, 281–306.

[5] a) D. M. Adams, A. Dei, A. L. Rheingold, D. N. Hendrickson, *Angew. Chem. Int. Ed. Engl.* **1993**, *32*, 880–882; b) D. M. Adams, A. Dei, A. L. Rheingold, D. N. Hendrickson, *J. Am. Chem. Soc.* **1993**, *115*, 8221–8229; c) O.-S. Jung, D. H. Jo, Y. A. Lee, B. J. Conklin, C. G. Pierpont, *Inorg. Chem.* **1997**, *36*, 19–24; d) O.-S. Jung, C. G. Pierpont, *J. Am. Chem. Soc.* **1994**, *116*, 2229–2230; e) O.-S. Jung, D. H. Lee, Y. S. Sohn, C. G. Pierpont, *Inorg. Chem.* **1998**, *37*, 5875–5880; f) S. Bin-Salamon, S. H. Brewer, E. C. Depperman, S. Franzen, J. W. Kampf, M. L. Kirk, R. K. Kumar, S. Lappi, K. Peariso, K. E. Preuss, D. A. Shultz, *Inorg. Chem.* **2006**, *45*, 4461–4467.

[6] S. Messaoudi, V. Robert, N. Guihéry, D. Maynau, *Inorg. Chem.* **2006**, *45*, 3212–3216 and references cited therein.

[7] a) W. R. Cullen, J. D. Woollins, *Coord. Chem. Rev.* **1981**, *39*, 1–30; b) C. G. Pierpont, C. W. Lange, *Prog. Inorg. Chem.* **1994**, *41*, 331; c) J. L. Reddinger, J. R. Reynolds, *Macromolecules* **1997**, *30*, 673–675; d) A. M. Costero, C. Andreu, R. Martínez-Mañez, J. Soto, L. E. Ochando, J. M. Amigó, *Tetrahedron* **1998**, *54*, 8159–8170; e) T. Hirao, *Coord. Chem. Rev.* **2002**, *226*, 81–91; f) C. Rovira, *Chem. Rev.* **2004**, *104*, 5289–5318.

[8] a) P. Gütlich, A. Dei, *Angew. Chem. Int. Ed. Engl.* **1997**, *36*, 2734–2736; b) A. Vlcek, *Comments, Inorg. Chem.* **1994**, *16*, 207–228; c) C. G. Pierpont, *Coord. Chem. Rev.* **2001**, *216*, 99–125.

[9] a) D. N. Hendrickson, C. G. Pierpont, *Top. Curr. Chem.* **2004**, *234*, 63–95; b) O. Sato, J. Tao, Y.-Z. Zhang, *Angew. Chem. Int. Ed.* **2007**, *46*, 2152–2187.

[10] a) D. Chang, T. Malinski, A. Ulman, K. M. Kadish, *Inorg. Chem.* **1984**, *23*, 817–824; b) J. Seth, V. Palaniappan, D. F. Bocian, *Inorg. Chem.* **1995**, *34*, 2201–2206.

[11] I. Ratera, D. Ruiz-Molina, F. Renz, J. Ensling, K. Wurst, C. Rovira, P. Gütlich, J. Veciana, *J. Am. Chem. Soc.* **2003**, *125*, 1462–1463.

[12] a) M. Li, D. Bonnet, E. Bill, F. Neese, T. Weyhenmüller, N. Blum, D. Sellmann, K. Wieghardt, *Inorg. Chem.* **2002**, *41*, 3444–3456; b) D. Herebian, P. Ghosh, H. Chun, E. Bothe, T. Weyhenmüller, K. Wieghardt, *Eur. J. Inorg. Chem.* **2002**, *8*, 1957–1967; c) K. Ray, E. Bill, T. Weyhenmüller, K. Wieghardt, *J. Am. Chem. Soc.* **2005**, *127*, 5641–5654; d) Y. Shimazaki, T. Yajima, F. Tani, S. Karasawa, K. Fukui, Y. Naruta, O. Yamauchi, *J. Am. Chem. Soc.* **2007**, *129*, 2559–2568.

[13] E. R. Altwicker, *Chem. Rev.* **1967**, *67*, 475–531.

[14] A. K. Nairn, R. Bhalla, S. P. Foxon, X. Liu, L. J. Yellowlees, B. C. Gilbert, P. H. Walton, *J. Chem. Soc., Dalton Trans.* **2002**, 1253–1255 and references cited therein.

[15] K. S. Min, T. Weyhermüller, K. Wieghardt, *Dalton Trans.* **2004**, 178–186 and references cited therein.

[16] a) O. Hayaishi, M. Nozaki, *Science* **1969**, *164*, 389–396; b) C. A. Tyson, A. E. Martell, *J. Am. Chem. Soc.* **1972**, *94*, 939–945; c) A. Y. Girgis, A. L. Balch, *Inorg. Chem.* **1975**, *14*, 2724–2727; d) L. A. deLaire, R. C. Haltiwanger, C. G. Pierpont, *Inorg. Chem.* **1989**, *28*, 644–650.

[17] a) S. K. Larsen, C. G. Pierpont, *J. Am. Chem. Soc.* **1988**, *110*, 1827–1832; b) A. Caneschi, A. Cornia, A. Dei, *Inorg. Chem.* **1998**, *37*, 3419–3421; c) O. Cador, F. Chabre, A. Dei, C. Sangregorio, J. Van Slageren, M. G. F. Vaz, *Inorg. Chem.* **2003**, *42*, 6432–6440.

[18] T. K. Paine, T. Weyhermüller, L. D. Slep, F. Neewe, E. Bill, E. Bothe, K. Wieghardt, P. Chaudhuri, *Inorg. Chem.* **2004**, *43*, 7324–7338.

[19] The redox activity of these ligands not only allows for the existence of valence tautomerism but also for additional switching capacities resulting from an electrochemical process. Such a strategy has been shown to be very useful for the systematic tuning of the critical temperature (T_c), at which there are equal amounts of both tautomers, as well as of the net magnetic moments and optical properties of the tautomeric isomers; a) D. Ruiz-Molina, L. N. Zakharov, A. L. Rheingold, D. N. Hendrickson, *J. Phys. Chem. Sol.* **2004**, *65*, 831–837; b) D. Ruiz-Molina, K. Wurst, D. Hendrickson, C. Rovira, J. Veciana, *Adv. Funct. Mater.* **2002**, *12*, 347–351; c) D. Ruiz-Molina, J. Veciana, K. Wurst, D. N. Hendrickson, C. Rovira, *Inorg. Chem.* **2000**, *39*, 617–619; d) D. Ruiz, J. Yoo, I. Guzei, A. L. Rheingold, D. N. Hendrickson, *Chem. Commun.* **1998**, 2089–2090.

[20] a) M. Kurihara, H. Nishihara, *Coord. Chem. Rev.* **2002**, *226*, 125–135; b) Y. Men, S. R. Korupoju, M. Kurihara, J. Mizutani, H. Nishihara, *Chem. Eur. J.* **2005**, *11*, 7322–7327; c) J. Yoshino, M. Kano, T. Kawashima, *Chem. Commun.* **2007**, 559–561; d) J. Přikryl, M. Černý, H. Bělohlavová, V. Macháček, A. Lyčka, *Dyes. Pigm.* **2007**, *72*, 392–402.

[21] W. Kaim, N. Doslik, S. Frantz, T. Sixt, M. Wanner, F. Baumann, G. Denniger, H.-J. Kümmerer, C. Duboc-Toia, J. Fiedler, S. Zalis, *J. Mol. Struct.* **2003**, *656*, 183–194.

[22] G. Speier, J. Csihony, A. M. Whalen, C. G. Pierpont, *Inorg. Chem.* **1996**, *35*, 3519–3524.

[23] a) F. Stunnenberg, H. Cerfontain, R. B. Rexwinkel, *Recl. Trav. Chim. Pays-Bas* **1992**, *111*, 438–447; b) G. Bauer, K. Scheffler, H. B. Stegmann, *Chem. Ber.* **1976**, *109*, 2231–2242.

[24] V. K. Bhardwaj, N. Singh, M. S. Hundal, G. Hundal, *Tetrahedron* **2006**, *62*, 7878–7886.

[25] K. Haghbeen, W. Tan, *J. Org. Chem.* **1988**, *63*, 4503–4505.

[26] a) C. Ruslim, K. J. Ichimura, *J. Mat. Chem.* **1999**, *9*, 673–681; b) K. Srinivasa, K. Abiraj, D. C. Gowda, *Tetrahedron Lett.* **2003**, *45*, 5835–5837.

[27] S. Patel, B. K. Mishra, *Tetrahedron Lett.* **2004**, *45*, 1371–1372.

[28] Q. Wang, Y. Yang, Y. Li, W. Yu, Z. T. Hou, *Tetrahedron Lett.* **2006**, *62*, 6107–6112.

[29] J. Vinsova, K. Cermakova, A. Tomeckova, M. Ceckova, J. Jampilek, P. Cermak, J. Kunes, M. Dolezal, F. Staud, *Bioorg. Med. Chem.* **2006**, *14*, 5850–5865.

[30] S. Yoshida, S. Shiokawa, K. Kawano, T. Ito, H. Murakami, H. Suzuki, Y. J. Sato, *Med. Chem.* **2005**, *48*, 7075–7079.

[31] P. Pattanayak, J. L. Pratihar, D. Patra, A. Burrows, M. Mohan, S. Chattopdhyay, *Eur. J. Inorg. Chem.* **2007**, *27*, 4263–4271, and references therein.

[32] N. Ventosa, D. Ruiz-Molina, J. Sedó, C. Rovira, X. Tomas, J.-J. André, A. Bieber, J. Veciana, *Chem. Eur. J.* **1999**, *5*, 3533.

Received: December 13, 2007